1984

TRANSIENT CHARACTERISTICS OF DENSE GAS DISPERSION, PART II:

Numerical Experiments on Dense Cloud Physics

By

Robert N. Meroney*

Prepared for Submission to

JOURNAL OF HAZARDOUS MATERIALS

Fluid Mechanics and Wind Engineering Program
Department of Civil Engineering
Colorado State University
Fort Collins, CO 80523

*Professor, Civil Engineering

CEP83-84RNM7b

DRAFT 21/12/83

TRANSIENT CHARACTERISTICS OF DENSE GAS DISPERSION, PART II:

Numerical Experiments on Dense Cloud Physics

By
Robert N. Meroney

ABSTRACT:

A depth-integrated quasi-three-dimensional numerical model (DENS20) is used to calculate the transient behavior of heavy and cold gas clouds. Numerical calculations with such a model provide an opportunity to examine dense cloud characteristics observed in the field but difficult to reproduce or measure accurately. The numerical model reveals the characteristics of upwind motion of dense gases at the source, gravity waves induced on the cloud top by wind shear, and the variable hazard zones associated with gases released instantaneously, over a finite time and continuously.

TRANSIENT CHARACTERISTICS OF DENSE GAS DISPERSION, PART II: Numerical Experiments on Dense Cloud Physics

By Robert N. Meroney

1.0 INTRODUCTION:

The use and transport of combustible hydrocarbon fuels having boiling points below ambient temperatures (liquified natural gas (LNG), ethane, propane or butane (LPG)) or similar storage and handling of toxic gases (ammonia, chlorine, sulfur dioxide, or hydrogen sulfide) invites questions concerning the consequences resulting from accidental release. Often such gases have molecular or temperature characteristics which result in negatively buoyant gas clouds which hug the ground and extend the hazard zone in time and space. This paper uses a depth-integrated numerical model (DENS20) to illuminate the fluid physics of dense plumes during periods of gravity-spread/air-entrainment dominance. Mechanistic details for this model and verification runs are provided in a Part I companion paper by Meroney (1984).

Systematic calculations with the physically realistic slab or primitive equations models provide an opportunity to examine transient plume characteristics often seen in the field but difficult to measure or reproduce. Morgan, Kansa, and Morris (1983) used a similar depth-integrated model (SLAB) to do a parameter variation study of heavy gas dispersion. They reported the response of hypothetical releases as source rate, wind speed, atmospheric stability, type of gas and source duration varied. A sensitivity study was performed to examine submodel choices for heat flux, surface drag, artifical diffusion, and entrainment model. They concluded that cold plume behavior is especially sensitive to surface heat transfer mechanisms and the level of plume turbulence assumed in the entrainment model. This paper will use the computationally fast DENS20 model to examine the following dense gas cloud characteristics:

a) Character of the upwind motion and breaking of the head wave,

b) Evidence for gravity waves on the cloud upper surface,

c) Source behavior during instantaneous, finite time, and continuous gas release, and

d) Shape of transient ignition zones.

The following sections describe the formulation of the depth-averaged model, its credibility based on comparison with some field experiments, and numerical experiments to respond to the points raised above.

2.0 A DEPTH-AVERAGED NUMERICAL MODEL:

A wind-tunnel calibrated, depth-integrated numerical model was used to calculate the behavior of heavy and cold gas clouds released into the atmosphere at ground level. The model (DENS20) is time dependent, quasi-three-dimensional, and permits cloud heating from below and the entrainment of moist air. The model does not depend upon the Boussinesq assumption, but it does require the hydrostatic assumption. In Meroney (1984) the model was verified by reproducing plume shape and concentration decay with distance and time for comparative cases from the Porton Downs (Picknett, 1981), China Lake (Koopman et al, 1982), and Colorado State University cold gas laboratory tests (Andriev, Neff, and Meroney, 1983) on dense gas behavior.

The plume properties (height, width, density, velocities, enthalpy, and concentration) are treated explicitly in their dependence on the downwind direction and on time, but they are averaged over crosswind sections. A sketch of a typical cloud at some instant in time, as assumed by the DENS20 model, is shown in Figure 1. The model consists of six coupled, partial differential equations which solve for plume width and section averaged height, density, enthalpy, lateral and longitudinal velocities, and mass fraction. The equations were developed in a difference form using an implicit, second-upwind-difference, donor-cell approach. The difference equations are solved by sequential use of the Thomas algorithm.

Formulae for the vertical and horizontal entrainment speeds, w_e and v_e, are based on perturbations of forms suggested by Eidsvik (1980) and Ermak et al (1982). Unspecified constants are determined by calibration of the model with laboratory data from Meroney and Lohmeyer (1982) and Neff and Meroney (1982). Expressions in the enthalpy conservation equation adjust for heat initially released when the cold plume entrains water vapor, but which is subsequently re-evaporated when the temperature of the plume exceeds ambient dew point. Surface heat transfer coefficients are predicted by an algorithm suggested by Leovy (1969) for mixed free and forced convection in the atmosphere. Alternative values for fully forced or fully free convection can also be used.

Readers interested in the details of model formulation are referred to Meroney (1983) or Meroney and Lohmeyer (1982). Other depth-averaged type models are described by Colenbrander (1980), Zeman (1982), and Morgan, Morris, and Ermak (1983).

3.0 NUMERICAL PREDICTION OF DENSE CLOUD PHYSICS:

Versions of the depth-integrated model designed to run in two-dimensional, radially symmetric, or laterally symmetric coordinate systems were used as appropriate to illuminate the dense cloud physics. The following sections examine each point in order.

3.1 Upwind Motion and Breaking of the Head Wave:

A two-dimensional version of the depth-integrated model was used to examine the effects of an opposing wind on the upwind cloud front. A two-dimensional square container of isothemal dense gas was realeased suddenly. Two cases are examined one for specific gravity $SG_o = 4.17$ and one for $SG_o = 1.2$ while maintaining the same approach flow.

Figures 2 and 3 display the variation of the dense gas cloud height ratio, H/HI, and concentration, χ , versus longitudinal location, X/HI, with time, t^*. (All values are dimensionless with HI and WI equal to initial plume height and longitudinal extent respectively, and dimensionless time, $t^* = tH_o^{-1/2}(g'_o)^{1/2}$. Concentration, χ , is expressed in mole fraction.) The cloud initially surges upwind, deepens at the upwind front as a result of the opposing fluid field and then shifts downwind. At long time the height distribution beconmes symmetric about the cloud center. More dilution takes place at the upwind edge of the cloud where the relative velocity of the wind about the cloud is greater.

Figures 4 and 5 display similar plots for the less dense cloud. In this case very little upwind movement occurs. The cloud moves only one cloud height upwind and then retreats downwind. The cloud attempts to send another gravity head upwind as the the upwind gas retreats and piles up on itself under the influence of the shear flow, but this again fails, and finally the cloud moves downwind as a semicircular cloud. The concentration curves suggest that, although larger relative velocites exist on the upwind side, there is relatively less surface over which to entrain. The greater cloud surface downwind presents an opportunity for more dilution even though it occurs at a smaller rate per unit are. Thus the concentration curves in Figures 3 and 5 slump in opposite directions.

3.2 Gravity Waves on the Upper Cloud Surface:

Plots of plume height, H/HI, versus radial location, R/RI, from a radially symmetric slab model calculation reveal an interesting cloud surface phenomenon. Figures 6 and 7 display progressive cloud profiles for calm and 0.2 m/sec wind speed conditions. The depth-averaged equations produce the appearance of a gravity head at early times; however, an elevated cloud nose cannot be produced by a depth-averaged approach...Notice that the long time cloud height is nearly

constant with radius and time for low wind speeds. The cloud grows more rapidly for finite wind speed conditions, because shear layer turbulence permits assymptotic lateral growth at a rate $V_g \approx u_*$, rather than $V_g \approx 1/R$.

Surface waves develop on the cloud top after about $t^* = 30$. One's first reaction might be that these waves are evidence of numerical instability; however, there is reason to believe the waves are actually a real phenomenon. Sketched on Figure 8 are typical plots of local radial density, ρ, and the cloud height, H, at some time greater than $t^* = 30$. Also displayed is the product ρH^2, which is the depth-averaged hydrostatic pressure. The product term has a maximum, which means fluid to the left of the maximum will be accelerated toward cloudlcenter, while fluid to the right of the center will be accelerated outward. The result is fluid moving toward cloud center as shown in the second sketch. As fluid piles up at the cloud center it produces local wave speed conditions which exceed the average fluid velocities, and a series of waves move outward. These waves grow in time as they induce additional pressure perturbations, high local velocities, and greater entrainment rates. The typical progression of cloud shapes calculated are shown at the bottom of Figure 8.

Picknett (1981) reported the presence of gravity wves during the Porton experiments. He notes:

> "Of special interest is the consistency in cloud height after the initial violent motion has subsided. ...In this slow expansion phase the surface of the disc of cloud is sometimes disturbed by regular undulations, 100-200 mm in amplitude, several meters in wavelength and traveling at perhaps 200 ms^{-1}, which may, perhaps, be gravity waves."

Picknett also commented on the "surprising" rate of cloud dilution after initial cloud collapse for such a low wind speed. He attributed this mixing to persistent cloud turbulence possibly aided by the gravity waves.

3.3 Surface Behavior During Instantaneous, Finite Time, and Continuous Gas Release

Puttock, Blackmore, and Colenbrander (1982) suggest that only Test 8 of the China Lake Burro LNG Spill Series can be considered a "borderline" instantaneous gas cloud, while all

other Burro tests behaved in a continuous or steady-state manner. Conditions for this case were selected to numerically evaluate the implications of instantaneous, finite time, or continuous source conditions. Since the wind speeds which existed during Burro 8 were quite small (1.8 ± 0.3 m/sec and decreasing) and the boiloff times short (107 sec), calculations were performed assuming that the entire cold gas volume was released instantaneously over the boiloff area (Figure 9), and then the calculations were repeated with the boiloff spread over the observed release time (Figure 10). Finally a plume was simulated which boiled off the maximum perceived LNG liquid-layer area continuously at an average rate equal to that occuring during the finite release scenario (Figure 11).

During the sudden release scenario the cloud almost immediately convects downwind, but during the finite time release the 5% isopleth is ound to the source until the end of the release time, whereas the 5% isopleth becomes parabolic with an open end downwind during a continuous situation. The continuous release appears most hazardous in terms of downwind advection of flammable gas; however then instantaneous release results in the widest plume iosopleth.

3.4 Shape of Transient Igniton Zones:

Meroney and Lohmeyer (1983b) studied the statistical characteristics of dense gas clouds released in an atmospheric-boundary-layer wind tunnel. They found that the maximum root-mean-square of the concentration fluctuations (standard deviation) could be related to the local mean concentration by $\overline{c'^2}/\overline{C_m}^2 = 0.02/\overline{C_m}$, where $\overline{C_m}$ is the maxium volume or mole fraction concentration measured at a given location. This empirical expression follows the functional form suggested by Chatwin (1981), but the constant is chosen to bound 95 % of the data taken by Meroney and Lohmeyer (1982). The constant should decrease with increasing plume Richardson number, but the trend of the data was not clear. In addition the concentration, C_m, may be considered distributed in a log-normal manner at low concentrations. Thus knowledge of the mean concentration, standard deviation, and probability distribution permits calculation of the ignition probability of gas, **P**. (**P** is the likelihood that a flammable gas mixture will exist at a given location during any instant of a dense gas spill.)

Table 1 proposes hazardous zones for the three release cases discussed in the section above. Naturally the hazard zones are most extensive for situations where the mean concentration is advected the greater distances. These predictions of hazard zones are probably still conservative because of the conservative nature of the standard deviation algorithm used. The mean concentration tabulated by Koopman, et al (1982) is for a 10 second sample average; whereas the

computer program may be considered to produce an ensemble average. If the Burro 8 test were repeated many times it is 95% likely that flammable gases would not be present beyond 650 m. Of course it is also possible that the gas may be contained in a flammable pocket and not attached to the main flammable plume.

Acknowledgements:

The author wishes to acknowledge support from the Institute Wasserbau III, University of Karlsruhe, F.R.G.; the von Humboldt Foundation, F.R.G.; and the Gas Research Institute, U.S.A..

REFERENCES:

Andreiev, G., Neff, D. E., and Meroney, R. N. (1983), Heat Transfer Effects During Cold Dese Gas Dispersion, Gas Research Institute Report No. GRI 83/0082, Chicago, Illinois,

Chatwin, P. C. (1981), The Statistical Description of the Dispersion of Heavy Gas Clouds, Report for Health and Saftey Executive, U.K., Contract No. 1189/01.01, 138 pp.

Colenbrander, G. W. (1980), A mathematical model for the transient behaviour of dense vapour clouds, 3rd Int. Symp. on Loss Prevention and Safety Promotion in the Process Industries, Basel, Switzerland, 29 pp.

Eidsvik, K. J. (1980), A Model for Heavy Gas Dispersion in the Atmosphere, Atmospheric Environment, Vol. 14, pp. 769-777.

Ermak, D. L., Chan, S. T., Morgan, D. L., and Morris, L. K. (1982), A comparison of dense gas dispersion model simulations with Burro series LNG spill test results, J. Hazardous Materials, Vol. 6, Nos. 1 and 2, pp. 129-160.

Koopman, R. P., Cederwall, R. T., Ermak, D. L>, Goldwire, H. C. Jr., Hogan, W. J., McClure, J. W., McRae, T. G., Morgan, D. L., Rodean, H. C., and Shinn, J. H. (1982),Analysis of Burro series 40 m^3 LNG spill experiments, J. Hazardous Materials, Vol. 6, Nos. 1 and 2, pp. 43-84.

Leovy, C. B. (1969), Bulk Transfer Coefficient for Heat Transfer, Jour. of Geophysical Research, Vol. 74, No. 13, pp. 3313-3321.

Meroney, R. N. (1983), Unsteady Behavior of a Simulated LNG Vapor Cloud Suddenly Released into a Wind-tunnel Boundary Layer, Proceedings of American Gas Association Transmission Conference, May 2-4, 1983, Seattle, Washington, 21 pp.

Meroney, R. N. (1984), Transient Characteristics of Dense Gas Dispersion, Part I: A Depth-Averaged Numerical Model, J. of Hazardous Materials, Vol. xx, No. xx, pp. xx-xx.

Meroney, R. N. and Lohmeyer, A. (1982), Gravity Spreading and Dispersion of Dense Gas Clouds Released Suddenly into a Turbulent Boudary Layer, Gas Research Insitute Report GRI 81/0025, Chicago, Illinois, U.S.A., 220pp.

Meroney, R. N. and Lohmeyer, A. (1983a), Prediction of Propane Cloud Dispersion by a Wind-tunnel-data Calibrated Box Model, accepted by J. Hazardous Materials, 33pp.

Meroney, R. N. and Lohmeyer, A. (1983b), Statistical Characteristics of Instantaneous Dense Gas Clouds Released in an Atmospheric Boundary Layer Wind Tunnel, accepted by J. Boundary-Layer Meteorology, 38 pp.

Morgan, D. L. Jr., Morris, L. K., and Ermak, D. L. (1983), SLAB: A Time-Dependent Computer Model for the Dispersion of Heavy Gases Released in the Atmosphere, Lawerence Livermore National Laboratory, Livermore, California, Report UCRL-53383, 15 pp.

Neff, D. E. and Meroney, R. N. (1982), The Behavior of LNG Vapor Clouds: Wind-tunnel Tests on the Modeling of Heavy Plume Dispersion, Gas Research Institute Report GRI 80/0145, Chicago, Illinois, U.S.A., 120 pp. (Data Appendix is GRI 80/0145.1, 161 pp.)

Picknett, R. G. (1981), Dispersion of Dense Gas Puffs Released in the Atmosphere at Ground Level, Atmospheric Environment, Vol. 15, pp. 509-525.

Puttock, J. S., Blackmore, D. R., and G. W. Colenbrander (1982), Field experiments on dense gas dispersion, J. Hazardous Materials, Vol. 6., Nos. 1 and 2, pp. 13-42.

Zeman, O. (1982), The Dynamics and Modeling of Heavier-than-air, Cold Gas Releases, Atmospheric Environment , Vol. 16, No. 4, pp. 741-751.

LIST OF SYMBOLS:

Symbols	Definitions
B	Plume width
c	Concentration fluctuation or wave speed
C	Concentration mole fraction
g'	Gravitational constant
HI	Initial plume height
H	Plume height
HS	Heavyside operator
ℓ_b	Buoyancy length scale
$\mathcal{P}$	Ignition probability
R	Cloud radius
Re	Reynolds number
	$(g'_o H)^{1/2} H/\nu_a$
Ri_*	Richardson number
	$(g'_o H_o)/u_*^2$
SG	Specific gravity
t	Time
T	Time scale
u, U	Velocity, velocity scale
u_*	Friction velocity
v_e, w_e	Entrainment velocities
V	Plume volume
V_g	Gravity spread velocity
WI	Initial plume width
χ	Mole fraction concentration
x, y, z	Coordinates
z_o	Surface roughness

ν	Kinematic viscosity
ρ	Density
$\bar{\Phi}$	Humidity

Subscripts

a	Ambient air conditions, or arrival time
d	Departure time
m	Maximum
med	Median
o,i	Initial value or ground level
R	Reference value
1,2	Lower and upper flammability limits

Superscripts

$\overline{\quad}$	Ensemble average
*	Dimensionless value

Table 1. Distances to Lower Flammability Limit Based on Mean Concentration or P ignition = 0.05, for Burro Run No. 8

Source Condition	$\bar{C}_m$ = 0.05		P ignition = 0.05	
	x_{LFL} (m)	t_a (sec)	x_{LFL} (m)	t_a (sec)
Field Data	340	200	---	---
Sudden Release (DENS 20)	330	130	657	280
Finite Time Release w_o = 0.098 m/s t_R = 107 sec (DENS 20)	280	180	650	330
Continuous Release w_o = 0.098 m/s (DENS 20)	280	180	653	355

All numerical calculations with surface heat transfer by mixed convection and 7% relative humidity.

LIST OF FIGURES:

Tables

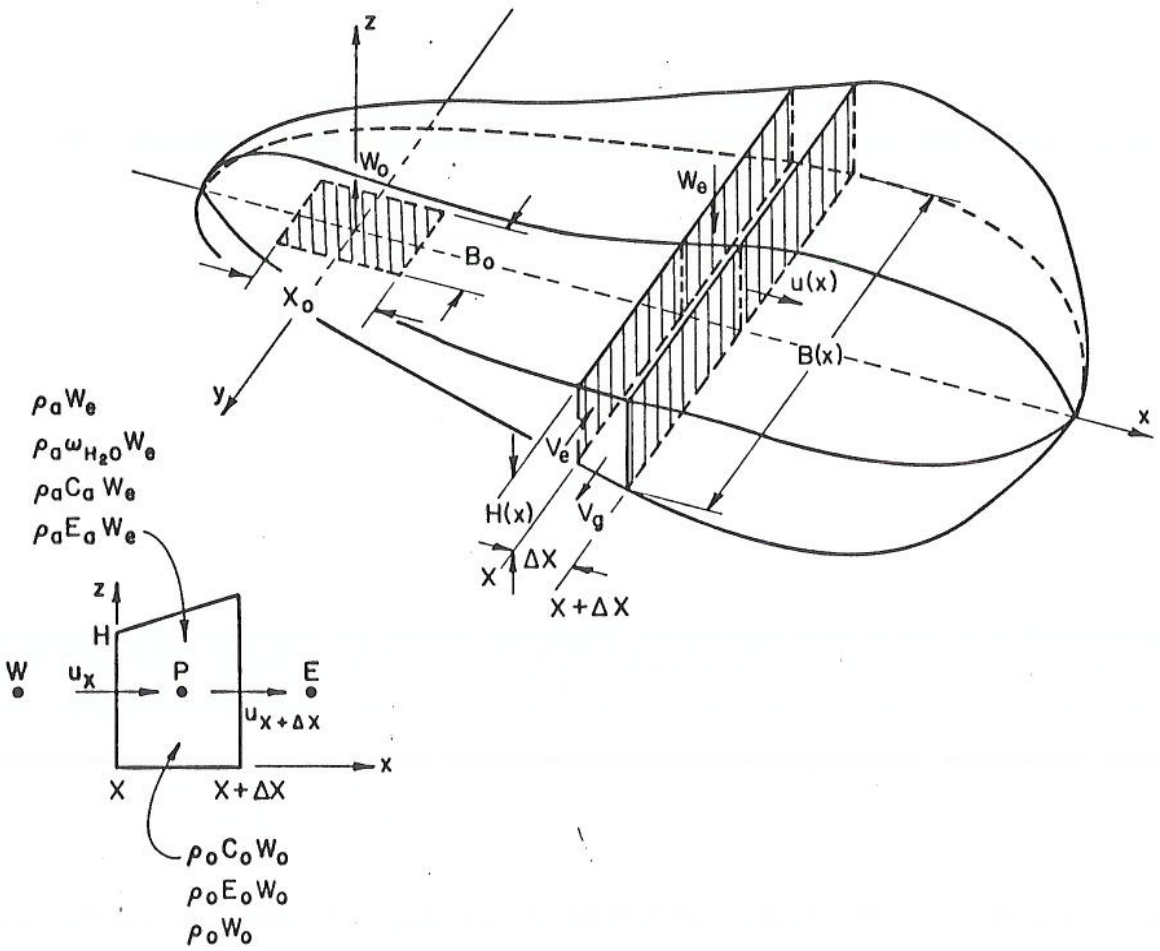

Figure 1. Control Volume for Depth-averaged Transport Equations

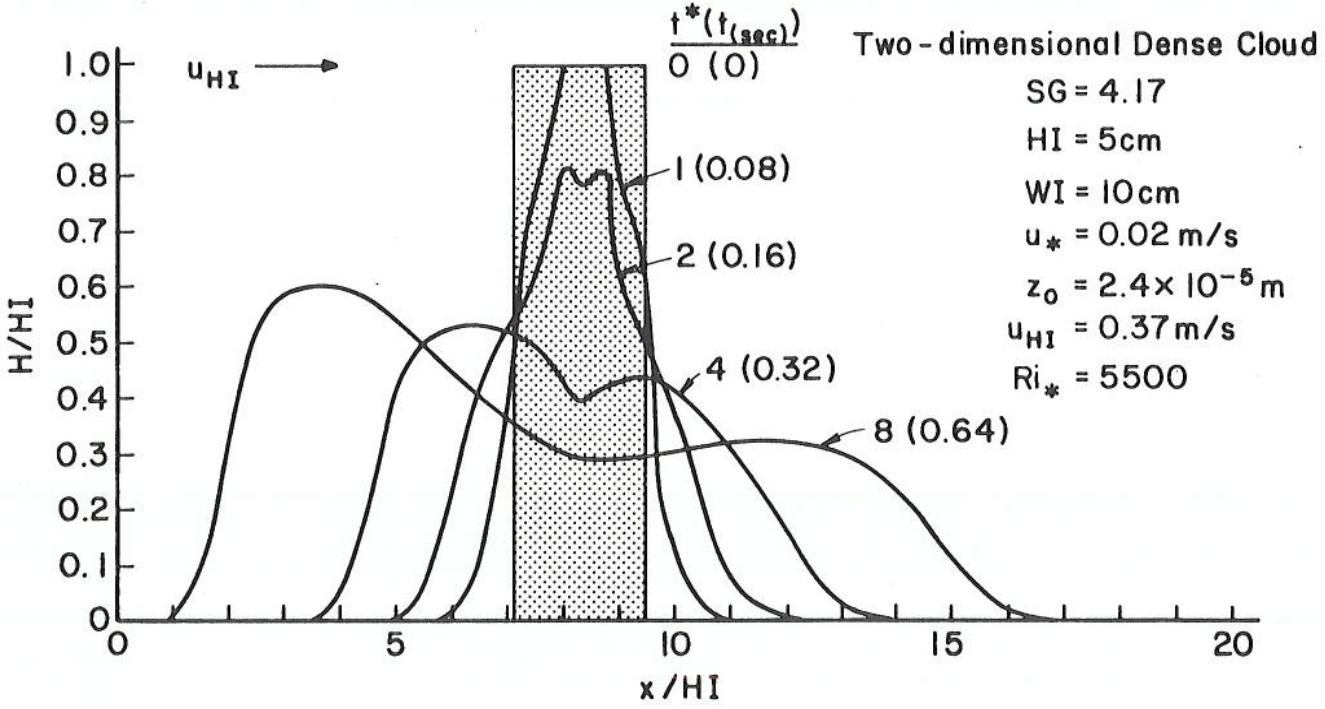

Figure 2. Transient 2-D Cloud Growth, SG = 4.17, u_R = 2 cm/sec, Ri_* = 5500

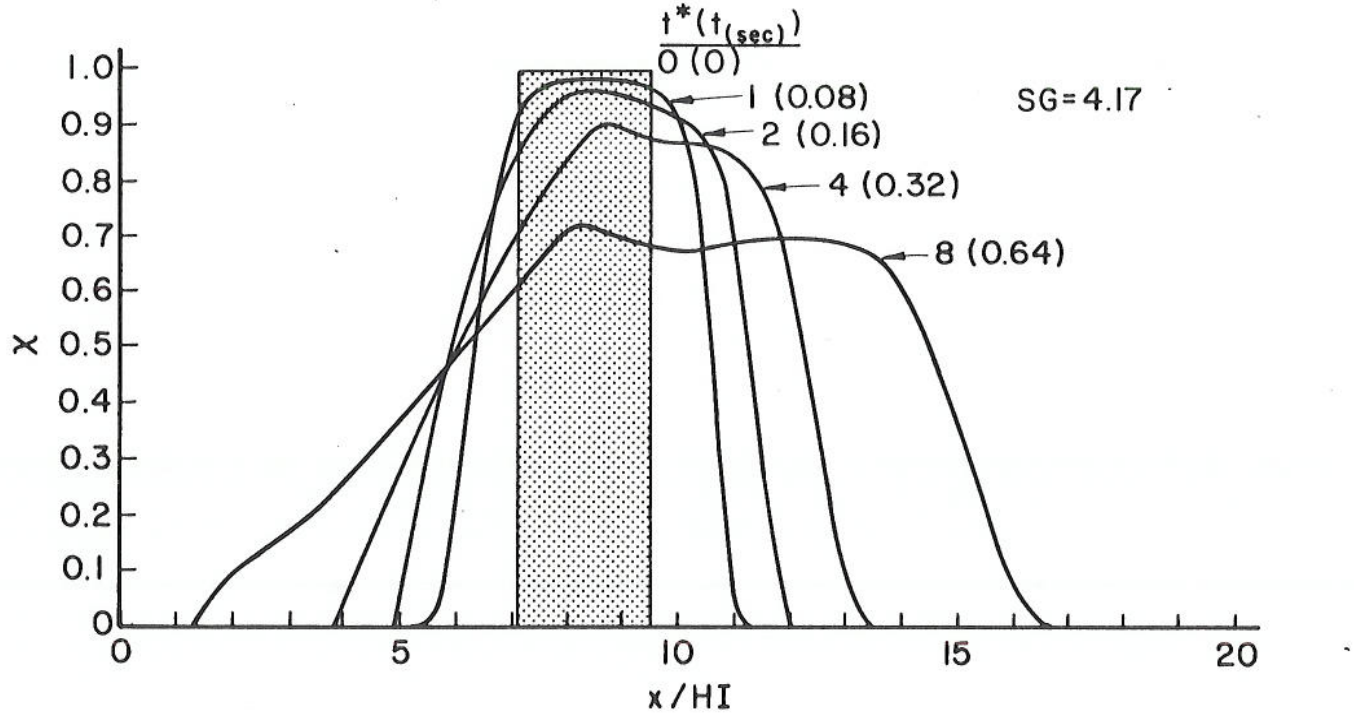

Figure 3 Transient 2-D Cloud Growth, SG = 4.17, u_R = 2 cm/sec, Ri_* = 5500

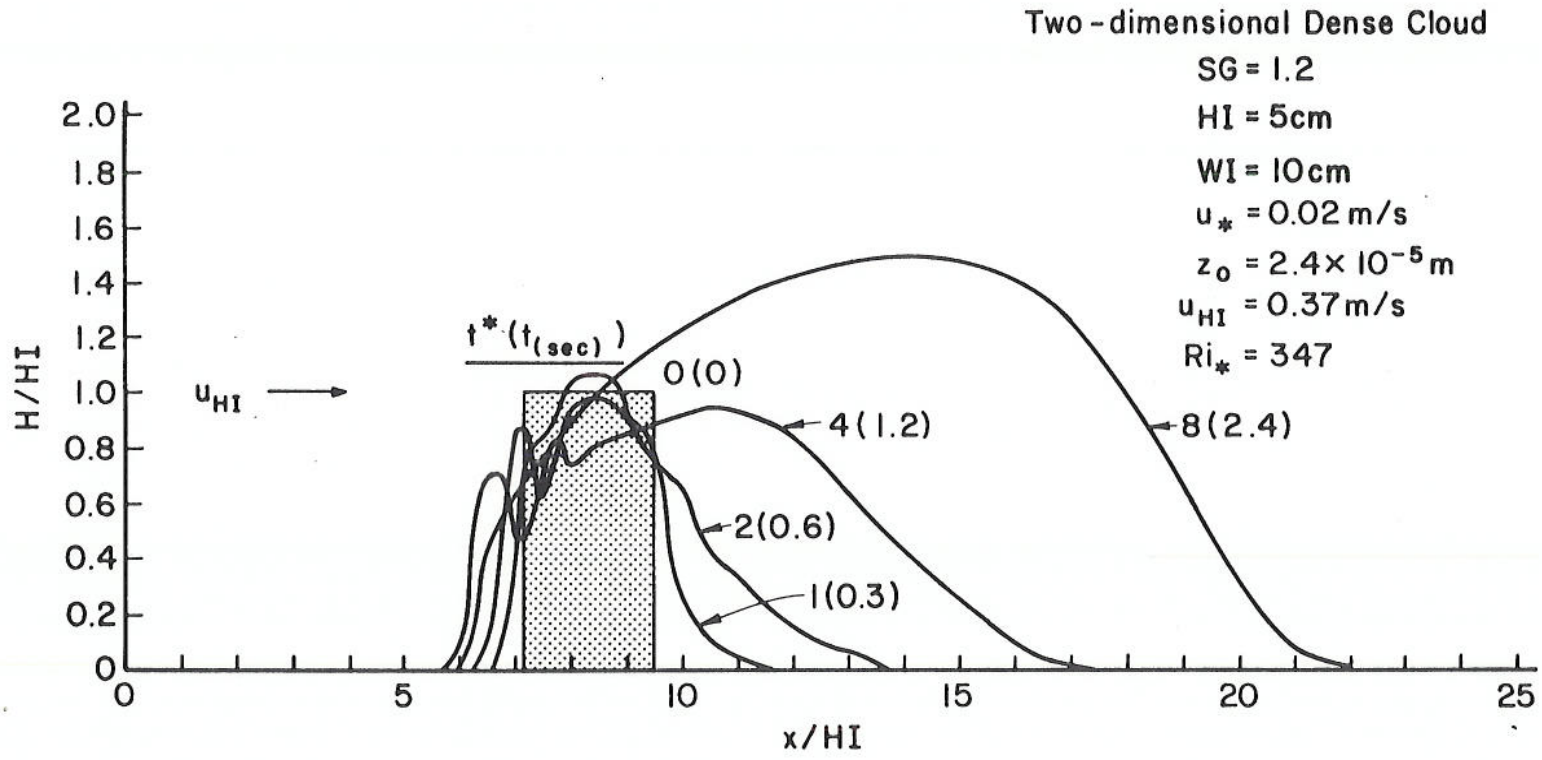

Figure 4 Transient 2-D Cloud Growth, SG = 1.2, u_R = 2 cm/sec, Ri_* = 347

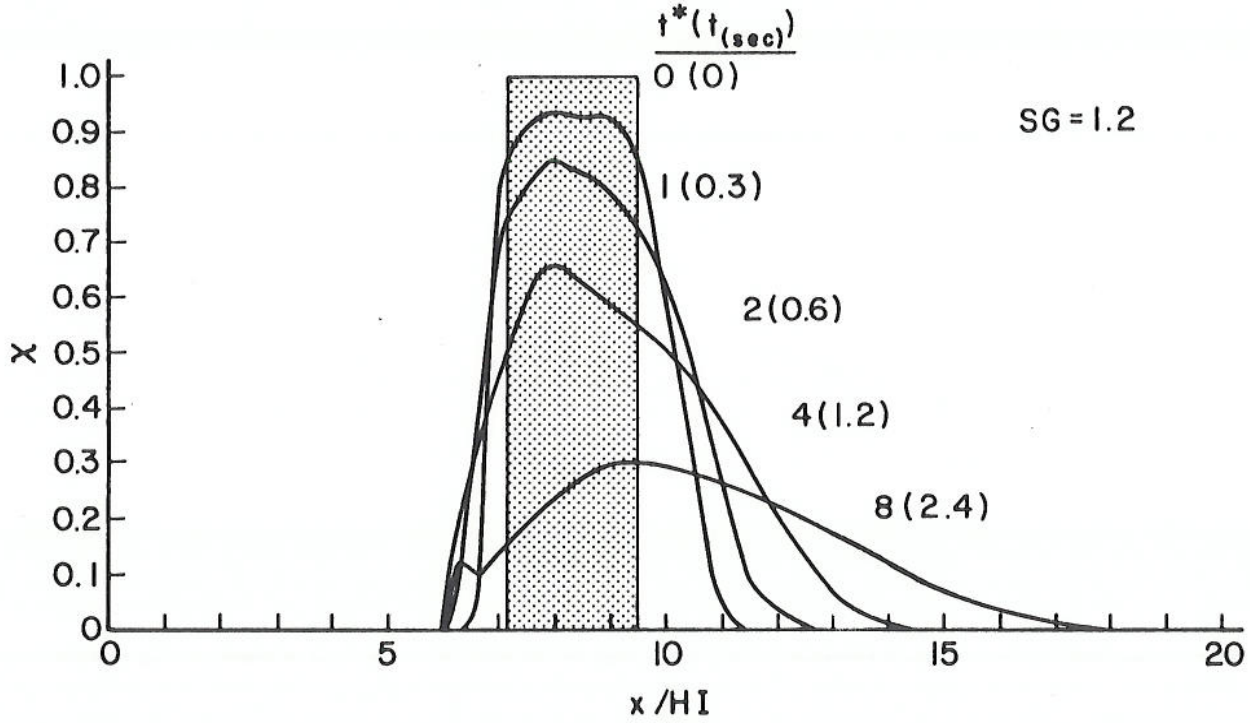

Figure 5 Transient 2-D Cloud Growth, SG = 1.2, u_R = 2 cm/sec, Ri_* = 347

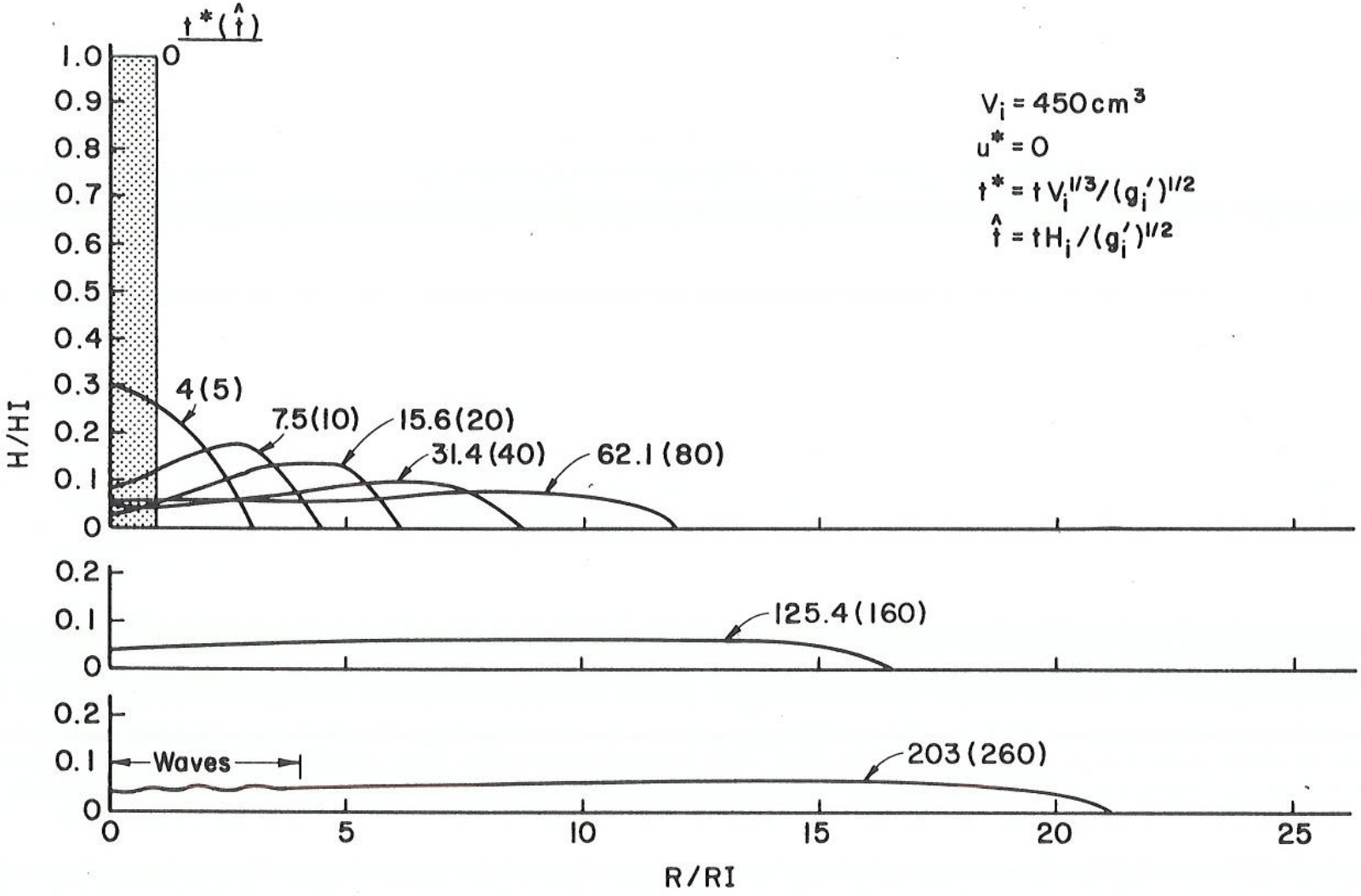

Figure 6 Cloud Height, H/HI, versus Radius, R/RI, $Ri_* = \infty$

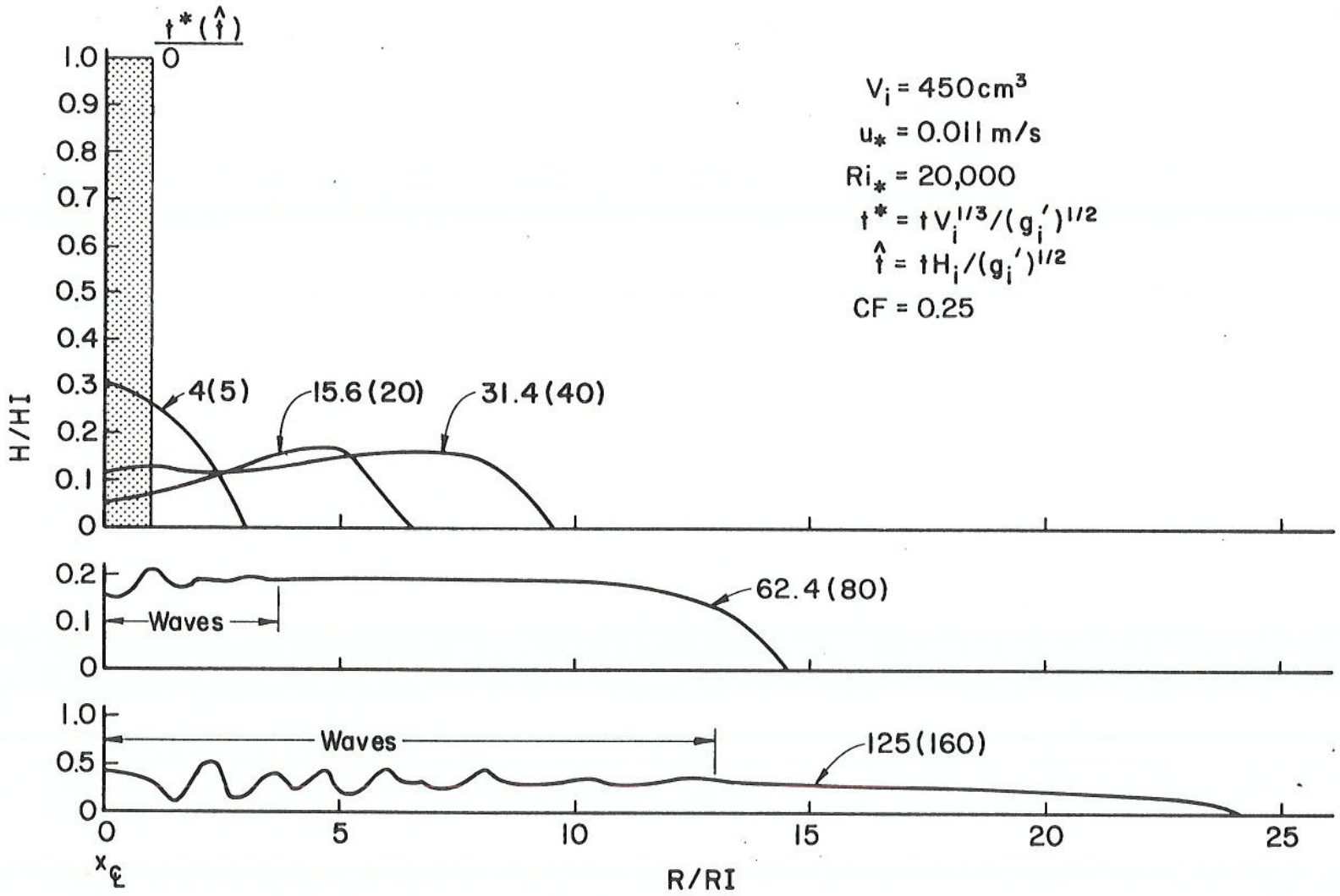

Figure 7 Cloud Height, H/HI, versus Radius, R/RI, $Ri_* = 20{,}000$

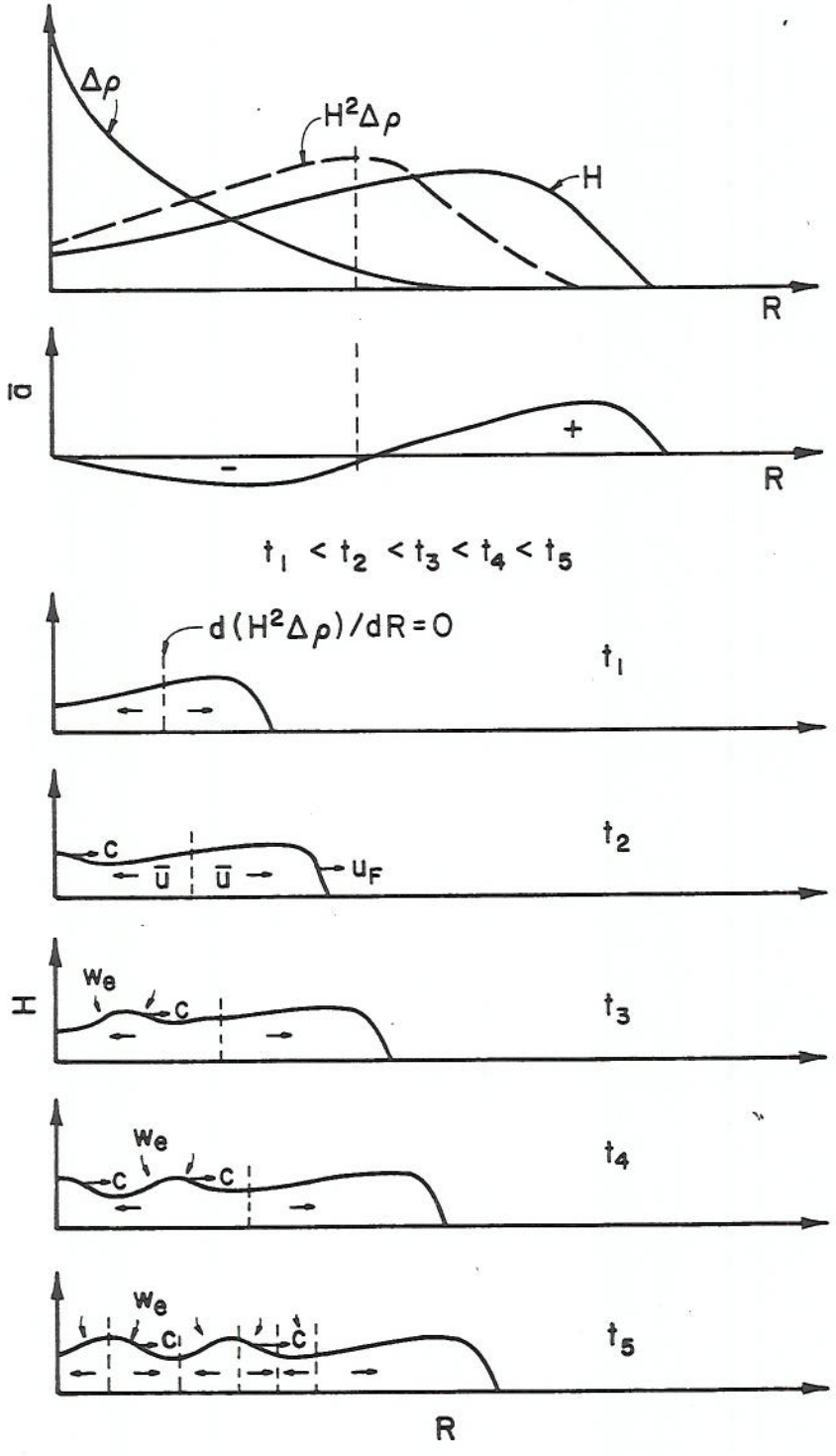

Figure 8 Physics of Surface Waves on Dense Clouds

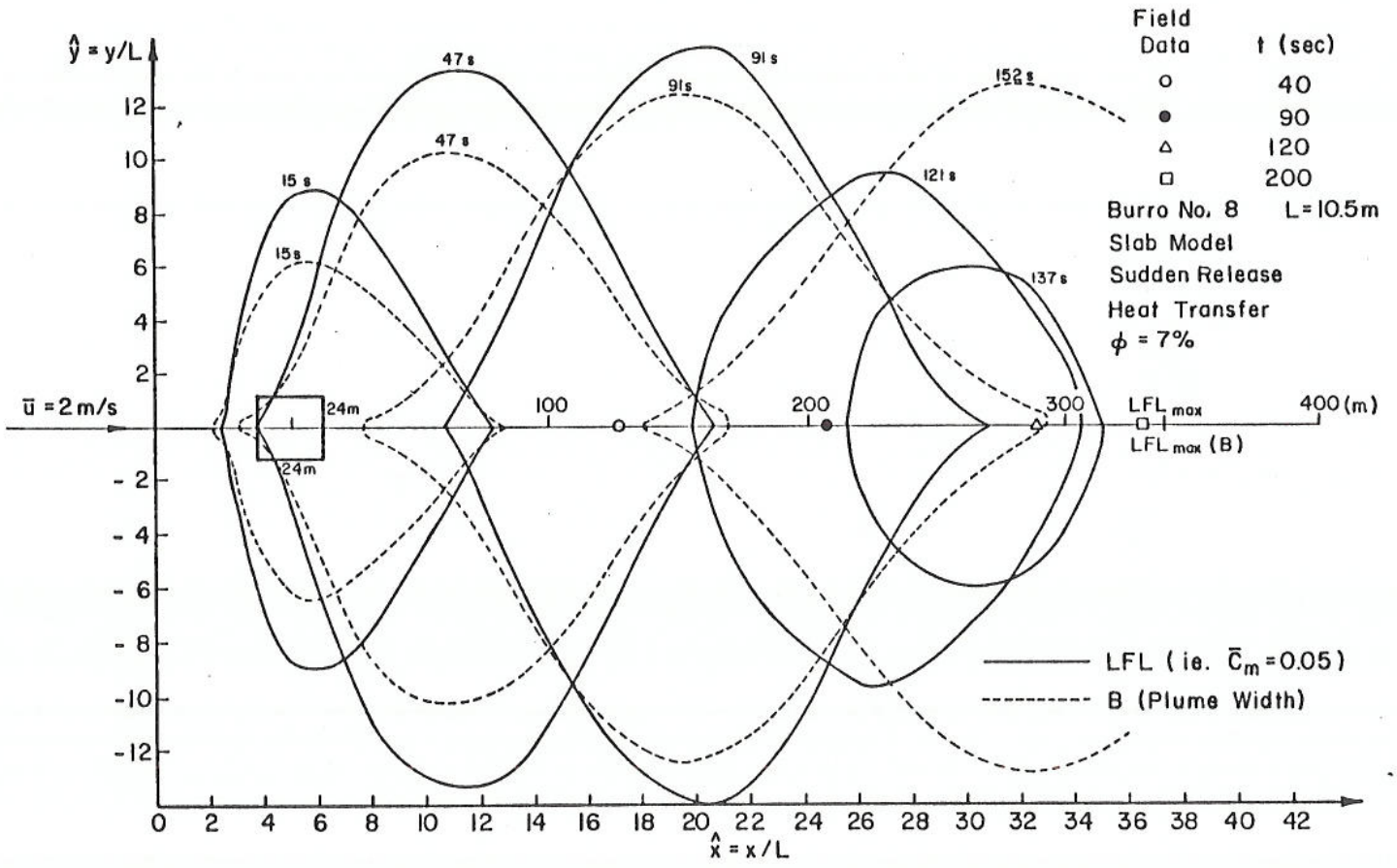

Figure 9. Burro Trial No. 8 - Transient Behavior of the LFL Mean Concentration of 5% Sudden Cloud Release

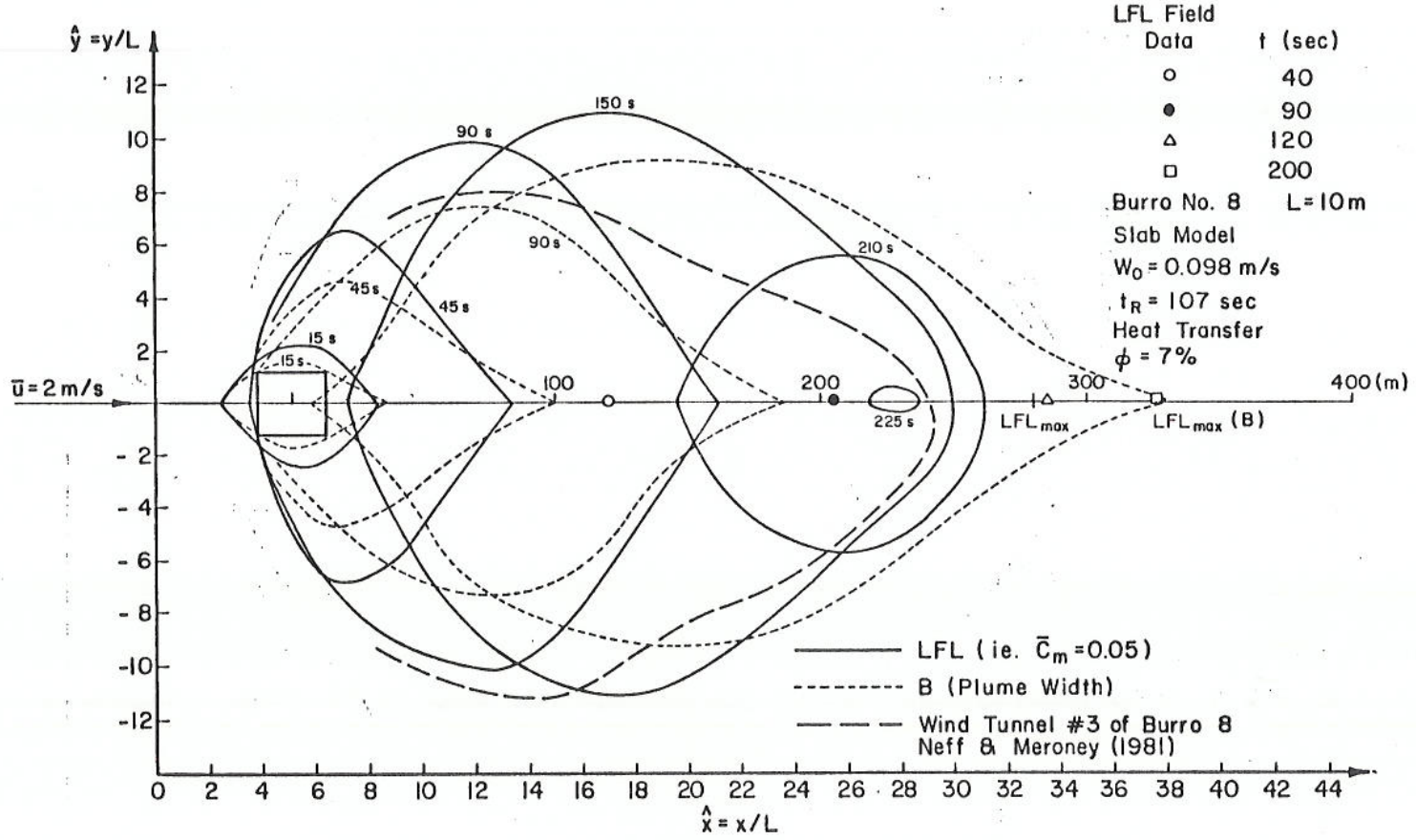

Figure *10*, Burro Trial No. 8 – Transient Behavior of the LFL Mean Concentration of 5% Finite Boiloff Time

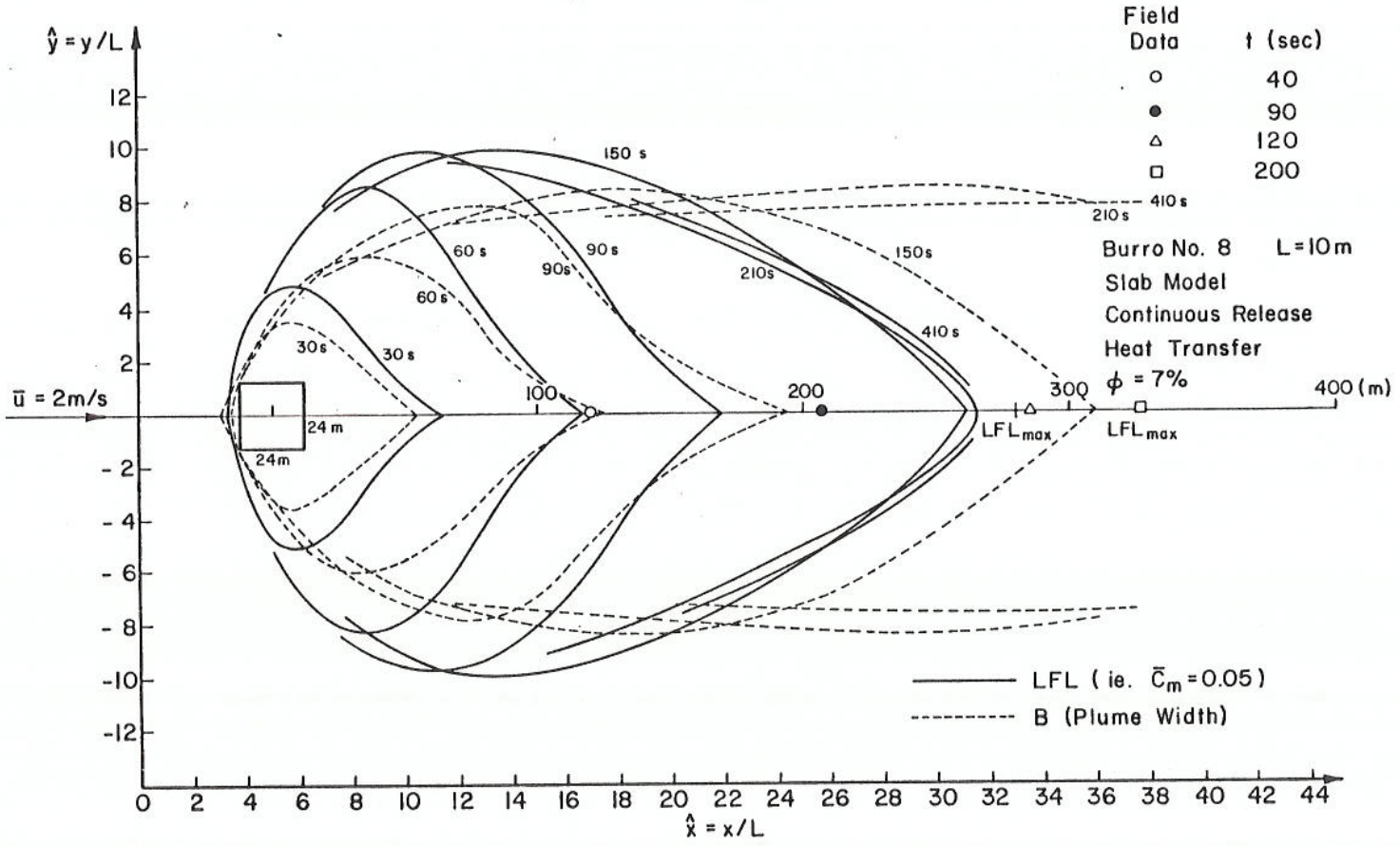

Figure 11 Burro Trial No. 8 - Transient Behavior of the LFL Mean Concentration of 5%, Continuous Boiloff